Journal of Luminescence 147 (2014) 190–195

Contents lists available at ScienceDirect

Journal of Luminescence

journal homepage: www.elsevier.com/locate/jlumin

Synthesis and photoluminescent properties of yttrium vanadate phosphor prepared by the non-hydrolytic sol–gel process

Marcela G. Matos [a], Emerson H. de Faria [a], Lucas A. Rocha [a], Paulo S. Calefi [a], Katia J. Ciuffi [a], Eduardo J. Nassar [a,*], Victor Hugo Vitorino Sarmento [b]

[a] Universidade de Franca, Av. Dr. Armando Salles Oliveira, 201 Franca, SP, CEP 14404-600, Brazil
[b] Universidade Federal de Sergipe, Av. Ver. Olimpio Grande s/n Itabaiana, SE, CEP 49500-000, Brazil

ARTICLE INFO

Available online 19 November 2013

Keywords:
YVO_4
Eu^{3+}
Non-hydrolytic sol–gel process
Luminescence

ABSTRACT

We used the non-hydrolytic sol–gel route to synthesize YVO_4 crystalline phases doped with europium III ion. We heat-treated the samples at 600, 800, and 1000 °C and characterized the materials by thermal analysis, X-ray diffraction, small-angle X-ray scattering, and photoluminescence. Larger weight loss occurred until 500 °C, ascribed to removal of residual precursor molecules. X-ray diffraction patterns evidenced YVO_4 phase formation at 600 °C. The crystallite size depended on the heat treatment temperature. SAXS showed that the nature of the system interfaces changed as a function of the thermal treatment. The excitation spectra of the samples displayed the charge transfer band. The photoluminescence data revealed the characteristic transition bands arising from the $^5D_0 \rightarrow {}^5F_J$ (J=0, 1, 2, 3, and 4) manifolds under maximum excitation at the charge transfer band and the $^5L_6$ level of the Eu^{3+} ion. The $^5D_0 \rightarrow {}^7F_2$ transition dominated the emission spectra, indicating that the Eu^{3+} ion occupies a site without inversion center. The lifetime and quantum efficiency values were about 0.70 ms and 50%, respectively, corroborating literature results.

1. Introduction

Inorganic matrixes doped with lanthanide ions (Ln^{3+}) find several applications in the areas of catalysis, luminescence devices, phosphors, optics, and electronics. The unique properties of lanthanides ions stem from incompletely filled 4f shell electrons. The 5s and 5p closed shells shield these electrons; consequently, they do not participate in bonding directly and interact with the environment much less strongly. The photololuminescent properties correspond to f→f transitions in the central ion [1,2]. They are important for high-definition television technology, which requires highly efficient, low-cost phosphors. For a material to be applied as phosphor, it must have high quantum efficiency, effective absorption and excitation, color purity, and long emission lifetime. Moreover, morphologic properties such as crystal size and shape, chemical composition, and surface features can affect the characteristics of the phosphors [3].

The lanthanide vanadate crystal ($LnVO_4$) belongs to the tetragonal $I4_1/amd$ spatial group [4]. Yttrium vanadates doped with trivalent lanthanide ions (YVO_4:Ln^{3+}, Ln^{3+}=Er^{3+}, Ho^{3+}, Nd^{3+}, Sm^{3+}, Yb^{3+}, Eu^{3+}, or Tm^{3+}) have interesting luminescent properties and can be potentially applied as TV phosphors, plasma display panels (PDPs), lamps, lasers, cathode ray tubes (CRTs), field emission displays (FEDs), X-ray detectors, and scintillators in medical image detectors [5–12].

Solid-state reactions [13,14], co-precipitation, [15,16] direct precipitation [9], microwave heating, [8,17] hydrothermal treatment [3,6,18], spray pyrolysis, [19–21] and the sol–gel process [11,22] are among the methodologies used to prepare YVO_4:Eu^{3+} or similar materials. A very efficient route to produce these materials is the non-hydrolytic sol–gel technique, which involves condensation of chloride precursors with alkoxides obtained in situ in non-aqueous media. The alkoxide originates from the reaction of halide precursors with oxygen donors (ethers, alcohols, etc.), which offers advantages such as high degree of condensation, absence of residual hydroxyl groups, high homogeneity, low reaction temperature, good stoichiometric control, short heating time, and commercially available reagents [2,23].

In this study, we employed the non-hydrolytic sol–gel methodology to prepare YVO_4:Eu^{3+}. We investigated the influence of temperature on the phase-purity of the material by thermal analyses, X-ray diffraction, small angle X-ray scattering, and transmission electron microscopy. We studied the luminescent properties of YVO_4:Eu^{3+} by photoluminescence of the Eu^{3+} ion, lifetime of the Eu^{3+} ion excited state, and quantum efficiency.

2. Experimental

2.1. Preparation of the lanthanide ion chloride ($LnCl_3$, $Ln=Eu^{3+}$ and Y^{3+}) and vanadium oxide chloride ($VOCl_2$) 1.10^{-1} mol L^{-1} solutions

First, the vanadium, yttrium, and europium oxides were calcined at 900 °C for 2 h. Then, 0.4547 g of V_2O_5, 0.5645 g of Y_2O_3,

* Corresponding author. Tel.: +55 16 3711 8871; fax: +55 16 3721 3266.
E-mail address: ejnassar@unifran.br (E.J. Nassar).

0022-2313/$ - see front matter © 2013 Elsevier B.V. All rights reserved.
http://dx.doi.org/10.1016/j.jlumin.2013.11.034

and 0.8798 g of Eu_2O_3 were dissolved in HCl 6.0 mol L^{-1}, followed by three additions of ethanol and subsequent evaporation. The concentration of the Ln^{3+} ion in the ethanolic solution was 1.10×10^{-1} mol L^{-1}.

2.2. Non-hydrolytic sol–gel synthesis of the $Y_2O_3(Eu_2O_3)$–V_2O_5 host

The host was synthesized by modification of the non-hydrolytic sol–gel method described by Acosta et al. [24] as reported by us [2,25–27]. To this end, 25.0 mL of $VOCl_2$, 24.8 mL of YCl_3, and 0.250 mL of $EuCl_3$ solutions were reacted with 15.0 mL of ethanol (EtOH). The lanthanide ion dopant (Eu^{3+}) was added at a molar ratio of 1% in relation to the Y^{3+} ion. The mixture was kept in a silicon oil bath at 100 °C for 4 h, under reflux (the condenser was placed in a thermostatic bath at −5 °C) and argon atmosphere. After the reflux, the mixture was kept in the mother liquor at room temperature (RT) overnight, to cool and age. The solvent was removed under vacuum. The powders were dried in a conventional oven at 100 °C and heat-treated at 600, 800, and 1000 °C for 4 h, in air.

2.3. Characterization techniques

Thermal analysis (TG/DTG) was carried out (Thermal Analyst 2100 – TA Instruments SDT 2960 simultaneous DTA-TG) in nitrogen atmosphere at a heating rate of 20 °C min^{-1}, from 25 to 1000 °C. The X-ray diffraction (XRD) measurements were performed at room temperature using a Rigaku Geigerflex D/max-c diffractometer with monochromated CuKα radiation ($\lambda = 1.54$ Å). Diffractoframs were recorded in the 2θ range from 4° to 80 ° at a resolution of 0.05°. SAXS measurements were conducted at the Brazilian Synchrotron Light Laboratory (LNLS). The incident X-ray monochromatic beam ($k = 1.488$ A °) was monitored by means of a photomultiplier and detected on a Pilatus detector (8 × 8 binning). The SAXS chamber parasitic scattering was also regidtered (with bias and dark-noise subtraction) and subtracted from the sample pattern after sample attenuation correction. Photoluminescence (PL) data were obtained under continuous Xe lamp (450 W) excitation using a spectrofluorometer (SPEX – Fluorolog II), at room temperature. The emission was collected at 90° from the excitation beam. The slits were placed at 1.0 and 0.2 mm for excitation and emission, respectively, giving a bandwidth of 3.5 and 0.5 nm. Oriel 58916 (exc.) and Corning 97612 (em.) filters were utilized. The morphology of the system was investigated by transmission electron microscopy (TEM) on a Joel-Jem 100 CXII electron microscope; a drop of powder suspension was deposited onto a copper grid prior to analysis.

3. Results and discussion

We recorded TG/DTG/DTA curves for the powders obtained by the non-hydrolytic sol–gel methodology followed by drying at 100 °C. The DTG curve displayed mass loss peaks at 60, 140, 245, 335, 380, 420, 660, and 790 °C, which corresponded to the loss of water molecules weakly bound to the oxide, solvent molecules, pyrolysis of organic matter remaining from the synthesis, and structural arrangement. The final mass loss occurred after 700 °C; the total mass loss was 40%. The DTA curve presented an exothermic peak at 660 °C, indicating that the oxide crystallized. No new exothermic peaks appeared until 1000 °C, so we dismissed the formation of a new phase, as the X-ray diffraction and photoluminescence spectra will confirm.

Fig. 1 depicts the XRD patterns of the samples after treatment at 600, 800, and 1000 °C for 4 h.

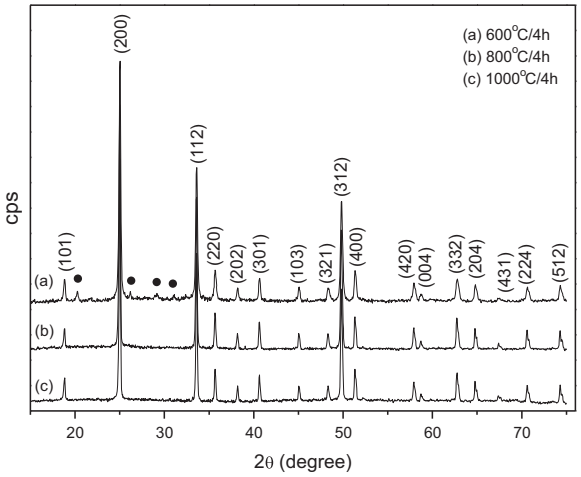

Fig. 1. X-ray diffraction patterns of the as-prepared powders after treatment at (a) 600, (b) 800, and (c) 1000 °C for 4 h, with the respective Miller index. The peaks marked with the symbol • correspond to impurities.

Table 1
Crystallite size for the samples treated at 600, 800, and 1000 °C for 4 h.

2θ (deg) ± 0.05°	Crystallite size (nm) ± 0.05 at 600 °C/4 h	Crystallite size (nm) ± 0.05 at 800 °C/4 h	Crystallite size (nm) ± 0.05 at 1000 °C/4 h
18.8	41.2	50.4	67.0
25.0	44.5	55.7	50.8
33.6	45.6	59.6	57.6
35.7	41.0	63.7	53.8
38.2	46.4	63.3	63.7
40.6	51.2	63.1	60.9
45.0	59.6	65.1	68.8
48.3	37.0	54.2	51.6
49.8	43.2	62.1	60.8
51.3	46.1	62.5	64.2
57.9	34.2	56.0	53.7
58.6	41.6	67.4	55.5
62.8	31.8	57.9	58.1
64.7	42.8	69.2	67.3
67.3	–	58.4	66.6
70.6	42.5	56.4	62.0
74.3	43.2	64.2	65.1

The XRD patterns of the samples treated at different temperatures exhibited well-defined peaks, ascribed to the tetragonal structure of the YVO_4 phase (JCPDS file no. 17-341). The sample treated at 600 °C displayed some low-intensity peaks, due to the presence of impurities or residual precursors of the syntheses. In the case of the samples treated at 800 and 1000 °C, the peaks relative to impurities disappeared, suggesting that only the crystalline phase YVO_4 existed in the samples. The XRD of the sample dried at 100 °C had a different phase from that observed for the samples treated at 600, 800, and 1000 °C; the XRD of the sample dried at 100 °C consisted of a mixture of the precursor chlorides.

We estimated the crystallite size by means of the Scherrer equation using the peak broadening of the XRD reflection [28]. Table 1 lists the crystallite size of the materials as a function of the heat treatment temperature.

Treatment at 600 °C for 4 h provided the smallest crystallites, evidencing that the crystallite size increased as a function of the heat treatment temperature. The average crystallite size was 43.2, 60.5, and 60.4 nm for the samples treated at 600, 800, and 1000 °C, respectively. Literature reports crystallite sizes of 45 and 40 nm for samples prepared at 800 and 1000 °C, respectively. [11,20]